directed towards design of inherently concurrent lossless decoders and Viterbi-type decoders. Such decoders should be capable of operating at high speed and should require marginal complexity increase as compared with the sequential decoders.

References

[1] K. K. Parhi and D. G. Messerschmitt, "Pipeline interleaving and parallelism in recursive digital filters, Part I: Pipelining using scattered look-ahead and decomposition," *IEEE Trans. Acoust., Speech, Signal Process.*, vol. 37, pp. 1099-1117, July 1989.

[2] —, "Pipeline interleaving and parallelism in recursive digital filt ers, Part II: Pipelined incremental block filtering," *IEEE Trans. Acoust., Speech, Signal Processing*, vol. 37, pp. 1118-1135, July 1989.

[3] D. A. Huffman, "A method for the construction of minimum redundancy codes," *Proc. IRE*, vol. 68, pp. 1098-1101, Sept. 1952.

[4] A. J. Viterbi, "Error bounds for convolutional codes and an asymptotically optimum decoding algorithm," *IEEE Trans. Inform. Theory*, vol. 13, pp. 260-269, Apr. 1967.

[5] G. D. Forney, "The Viterbi algorithm," *Proc. IEEE*, vol. 61, pp. 268-278, Mar. 1973.

[6] K. K. Parhi, "Algorithm transformation techniques for concurrent processors," *Proc. IEEE*, vol. 77, pp. 1879-1895, Dec. 1989.

[7] H. D. Lin and D. G. Messerschmitt, "Improving the iteration bound of finite state machines," in *Proc. IEEE Int. Symp. Circuits and Systems*, pp. 1328-1331, May 1989.

[8] H. D. Lin and D. G. Messerschmitt, "High throughput reconstruction of Huffman-coded images," in *Proc. IEEE Conf. Computer Design*, Oct. 1989.

[9] K. K. Parhi, "High-speed Huffman decoder architectures," in *Proc. 25th Asilomar Conf. Signals, Systems, and Computers*, Nov. 1991.

[10] G. Fettweis and H. Meyr, "Parallel Viterbi decoding by breaking the compare-select feedback bottleneck," in *Proc. IEEE Int. Conf. Communications*, pp. 719-723, June 1988.

[11] C. Y. Chang and K. Yao, "Viterbi decoding by systolic array," in *Proc. Ann. Allerton Conf. Communications, Controls, and Computing*, pp. 430-439, Oct. 1985.

[12] H. Thapar and J. Cioffi, "A block processing method for designing high-speed Viterbi decoders," in *Proc. IEEE Int. Conf. Communications*, pp. 836-840, 1989.

[13] K. K. Parhi, "Pipelining in dynamic programming architectures," *IEEE Trans. Signal Processing*, vol. 39, pp. 1442-1450, June 1991.

[14] —, "Look-ahead in dynamic programming and quantizer loops," in *Proc. IEEE Int. Symp. Circuits and Systems*, pp. 1382-1387, May 1989.

[15] G. Fettweis, L. Thiele, and H. Meyr, "Algorithm transformations for unlimited parallelism," in *Proc. 1990 IEEE Int. Symp. on Circuits and Systems*, pp. 1165-1169, May 1990.

Applications of Complex Filters to Realize Three-Dimensional Combined DFT/LDE Transfer Functions

L. T. Bruton and N. R. Bartley

Abstract—**The recently proposed method of combined discrete Fourier transform (DFT)/linear difference equation (LDE) filtering of three-dimensional (3-D) spatio-temporal signals employs LDE's with real coefficients. It is shown here that the real-coefficient LDE's impose transfer function symmetries that prevent the 3-D filter from distinguishing between 3-D input signals having reflective symmetry in the direction of the LDE filtering. These transfer function symmetry constraints are relaxed by using complex-coefficient LDE's.**

Manuscript received October 5, 1991.

The authors are with the Department of Electrical and Computer Engineering, University of Calgary, Calgary, AB, Canada T2N-1N4.

IEEE Log Number 9201435.

I. Introduction

The method of combined discrete Fourier transform (DFT)/linear difference equation (LDE) filtering has been proposed for the enhancement of multidimensional (MD) digital signals [1]. As shown in Fig. 1, the method operates on a 3-D input signal $x(n_1, n_2, n_3)$ by applying the two-dimensional (2-D) DFT on $x(n_1, n_2, n_3)$, performing 1-D LDE filtering of the resulting complex 2-tuple frequency points and then by applying the 2-D inverse DFT to the outputs of the LDE's. This method has applications in the enhancement of dynamic 2-D images.

The combined DTF/LDE method employs LDE's that have *real* coefficients. In this paper, we show for the 3-D case that LDE's with real coefficients impose a symmetry constraint on the frequency response $H(j\omega_1, j\omega_2, j\omega_3)$ that can be relaxed by employing LDE's having *complex* coefficients. Assuming spatial variables n_1, n_2 and a temporal variable n_3, with LDE filtering in the n_3 direction [1], LDE's having real coefficients lead to output images $y(n_1, n_2, n_3)$ in Fig. 1 having identical responses for both $x(n_1, n_2, n_3)$ and the *time-reversed* image $x(n_1, n_2, -n_3)$. It is shown here that this limitation may be overcome by employing LDE's with complex coefficients.

II. Transfer Function Symmetry Imposed on $H(j\omega_1, j\omega_2, j\omega_3)$ by LDEs Having Real Coefficients

We assume combined DFT/LDE filters where the 2-D DFT is performed over ω_1 and ω_2 ($\omega_{1,2} \epsilon \mathbb{Z}^2$) and 1-D continuous frequency domain (LDE) filtering in the direction n_3 ($\omega_3 \epsilon \mathbb{R}^1$). The overall input–output frequency response of the 3-D combined 2D-DFT/LDE filter is written as $H(j\omega_1, j\omega_2, j\omega_3) = M(\omega_1, \omega_2, \omega_3) < \Phi(\omega_1, \omega_2, \omega_3)$, where ω_1, ω_2, ω_3 belong to the 3-D frequency space Ω^3 that is discrete in ω_1, ω_2 and continuous in ω_3; that is, $\Omega^3 = \mathbb{Z}^2 \times \mathbb{R}^1$. For *real* input signals $x(n_1, n_2, n_3)$, and *identical real-coefficient* LDE's at each pair of 2-tuples (ω_1, ω_2) and $(-\omega_1, -\omega_2)$, the DFT operation imposes the following symmetry constraints [2]:

$$H(j\omega_1, j\omega_2, j\omega_3) = H(-j\omega_1, -j\omega_2, j\omega_3) \tag{1}$$

implying magnitude centro-symmetry (MCS) and phase centro-antisymmetry (PCAS) [3] over (ω_1, ω_2). The output signal $y(n_1, n_2, n_3)$ is *real* [1]. Consider the eight octants in Ω^3. From (1), the DFT operation constrains them into four pairs of MCS/PCAS octants, as follows:

$$\begin{aligned} H(j\omega_1, j\omega_2, j\omega_3) &= H(-j\omega_1, -j\omega_2, j\omega_3) \\ H(j\omega_1, j\omega_2, -j\omega_3) &= H(-j\omega_1, -j\omega_2, -j\omega^3) \\ H(j\omega_1, -j\omega_2, j\omega_3) &= H(-j\omega_1, j\omega_2, j\omega_3) \\ H(j\omega_1, -j\omega_2, -j\omega_3) &= H(-j\omega_1, j\omega_2, -j\omega_3) \\ &\text{independent octant-pairs} \\ &\text{in } \Omega^3 \text{ due to DFT operations} \end{aligned} \tag{2}$$

If the LDE filters on ω_3 have *real* coefficients, the following *additional* symmetry constraint applies to ω_3:

$$H(j\omega_1, j\omega_2, j\omega_3) = H(j\omega_1, j\omega_2, -j\omega_3) \quad \begin{array}{l}\text{additional octant} \\ \text{constraints in } \Omega^3 \text{ due} \\ \text{to real LDE coefficients.}\end{array} \tag{3}$$

Combining (2) and (3), $H(j\omega_1, j\omega_2, j\omega_3)$ is constrained as fol-

1057-7130/92$03.00

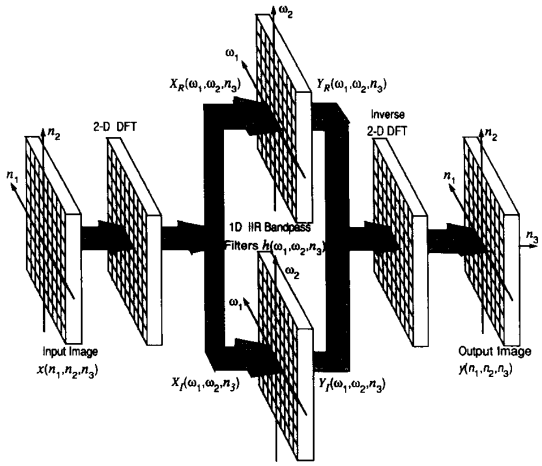

Fig. 1. 3-D combined DFT/LDE filtering method.

lows:

$$\begin{aligned} H(j\omega_1, j\omega_2, j\omega_3) &= H(-j\omega_1, -j\omega_2, j\omega_3) \\ &= H(j\omega_1, j\omega_2, -j\omega_3) \\ &= H(-j\omega_1, -j\omega_2, -j\omega_3) \\ H(j\omega_1, -j\omega_2, j\omega_3) &= H(-j\omega_1, j\omega_2, j\omega_3) \\ &= H(j\omega_1, -j\omega_2, -j\omega_3) \\ &= H(-j\omega_1, j\omega_2, -j\omega_3). \end{aligned} \tag{4}$$

Thus, only two of the eight octants are independent, and the remaining six are constrained by symmetry. Although (4) allows the magnitude response $M(\omega_1, \omega_2, \omega_3)$ to have *quadrantal symmetry* in (ω_1, ω_2), it does enforce the following type of symmetry over ω_3 that is undesirable in some practical situations.

Consider an input signal $x(n_1, n_2, n_3) \leftrightarrow X(j\omega_1, j\omega_2, j\omega_3)$ and a second, different input signal $x_1(n_1, n_2, n_3) \leftrightarrow X_1(j\omega_1, j\omega_2, j\omega_3)$ such that $x_1(n_1, n_2, n_3) \equiv x(n_1, n_2, -n_3)$, corresponding to a time-reversed version of $x(n_1, n_2, n_3)$. We therefore have

$$\begin{aligned} y(n_1, n_2, n_3) &\leftrightarrow Y(j\omega_1, j\omega_2, j\omega_3) \\ &= X(j\omega_1, j\omega_2, j\omega_3) H(j\omega_1, j\omega_2, j\omega_3) \end{aligned} \tag{5a}$$

$$\begin{aligned} y_1(n_1, n_2, n_3) &\leftrightarrow Y_1(j\omega_1, j\omega_2, j\omega_3) \\ &= X_1(j\omega_1, j\omega_2, j\omega_3) H(j\omega_1, j\omega_2, j\omega_3). \end{aligned} \tag{5b}$$

The DFT has the property that $X_1(j\omega_1, j\omega_2, j\omega_3) = X(j\omega_1, j\omega_2, -j\omega_3)$ so that (5b) may be written as

$$Y_1(j\omega_1, j\omega_2, j\omega_3) = X(j\omega_1, j\omega_2, -j\omega_3) H(j\omega_1, j\omega_2, j\omega_3). \tag{6}$$

From (3) and (6), we may write

$$Y_1(j\omega_1, j\omega_2, j\omega_3) = X(j\omega_1, j\omega_2, -j\omega_3) H(j\omega_1, j\omega_2, -j\omega_3) \tag{7}$$

and therefore, from (5a) and (5b),

$$Y_1(j\omega_1, j\omega_2, j\omega_3) = Y(j\omega_1, j\omega_2, -j\omega_3). \tag{8}$$

Taking the inverse 2-D DFT of (8) over (ω_1, ω_2) and then the inverse Fourier transform over ω_3 leads directly to the required result that

$$y_1(n_1, n_2, n_3) = y(n_1, n_2, -n_3) \tag{9}$$

implying that, *for a 3-D combined DFT/LDE filter with real-coefficient LDE's, time-reversal of the input leads to a corresponding time-reversal of the output.*

It is interesting to note that real-coefficient 3-D LDE filters and the 3-D DFT do not suffer from this limitation because they are only constrained as follows:

$$H(j\omega_1, j\omega_2, j\omega_3) = H(-j\omega_1, -j\omega_2, -j\omega_3) \tag{10}$$

implying four independent octants having MCS/PCAS in $(\omega_1, \omega_2, \omega_3)$.

Example: 3-D Frequency-Planar (FP) Filters using Real-Coefficient LDE's [4]

Frequency-planar (FP) filters have been used to selectively enhance *linear-trajectory* spatio-temporal signals, using real-coefficient LDE's with identical LDE's at each pair of 2-tuples (ω_1, ω_2) and $(-\omega_1, -\omega_2)$. They are implemented using narrow-band bandpass LDE's having center frequencies ω_3 where the passband surrounds the plane [4]

$$\alpha_1\omega_1 + \alpha_2\omega_2 + \alpha_3\omega_3 = 0 \qquad \boldsymbol{P}_1. \tag{11}$$

The magnitude transfer function $M(\omega_1, \omega_2, \omega_3)$ is unity on $\boldsymbol{P}_1$ and ideally rolls off rapidly to zero outside $\boldsymbol{P}_1$. However, according to (3), there must exist a second passband plane

$$\alpha_1\omega_1 + \alpha_2\omega_2 - \alpha_3\omega_3 = 0 \qquad \boldsymbol{P}_2 \tag{12}$$

because $M(\omega_1, \omega_2, \omega_3) = M(\omega_1, \omega_2, -\omega_3)$. If the passband $\boldsymbol{P}_1$ selectively transmits the linear trajectory signal $x(n_1, n_2, n_3)$, then the passband $\boldsymbol{P}_2$ selectively transmits the time-reversed signal $x(n_1, n_2, n_3) = x(n_1, n_2, -n_3)$. Ideally, we would like to remove the second passband $\boldsymbol{P}_2$ because we often want to enhance a linear-trajectory signal, but not a signal on the time-reversed trajectory.

III. The Design and Application of Complex-Coefficient LDE's

It is now shown that combined DFT/LDE filters can be designed so that $H(j\omega_1, j\omega_2, j\omega_3)$ has four *independent octants* by allowing the LDE filters to have *complex* coefficients. Let $T(j\omega_1, j\omega_2, j\omega_3)$ represent the frequency response of the 1-D complex-coefficient LDE filter on ω_3 at the 2-tuple (ω_1, ω_2). We select complex-coefficient LDEs at each pair of 2-tuples (ω_1, ω_2) and $(-\omega_1, -\omega_2)$ such that the corresponding frequency responses over ω_3 are complex conjugates; that is, so that

$$T(j\omega_1, j\omega_2, j\omega_3) = T(-j\omega_1, -j\omega_2, -j\omega_3). \tag{13}$$

Therefore, (2) remains in effect but (3) does not apply, and *four of the eight octant are independent.*

Complex Bandpass LDE Filters

Using *complex-coefficient LDE's*, we often require complex bandpass filters $T(j\omega_1, j\omega_2, j\omega_3)$ at each 2-tuple (ω_1, ω_2) having the *idealized* magnitude response $M(\omega_1, \omega_2, \omega_3)$ shown in Fig. 2.

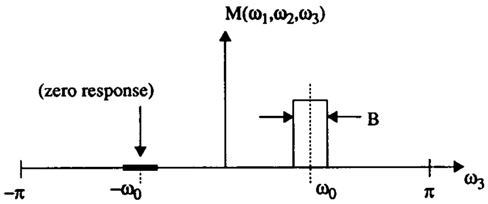

Fig. 2. Ideal Complex bandpass filter response.

A straightforward approach to the design of these 1-D complex filters is to employ the following discrete-domain method (which is equivalent to that described in [5] for the case of continuous-domain complex filters). We choose a suitable discrete-domain real-coefficient LDE corresponding to the low-pass filter $T(z)$, expressed in the factored form as

$$T(z) = \prod_{i=0}^{M-1} (z + \bar{a}_i) \Big/ \prod_{i=0}^{N-1} (z + \bar{b}_i), \tag{14}$$

where $\bar{a}_i = a_{Ri} + ja_{Ii}$ and $\bar{b}_i = b_{Ri} + jb_{Ii}$ are the zeros and poles, respectively. The transfer function of the required complex bandpass filter is then obtained by rotating $\bar{a}_i$ and $\bar{b}_i$ in the complex z-plane by equal angles ω_0 rad according to

$$\begin{bmatrix} a'_{Ri} \\ a'_{Ii} \end{bmatrix} = \begin{bmatrix} \cos\omega_0 & -\sin\omega_0 \\ \sin\omega_0 & \cos\omega_0 \end{bmatrix} \begin{bmatrix} a_{Ri} \\ a_{Ii} \end{bmatrix},$$

$$\begin{bmatrix} b'_{Ri} \\ b'_{Ii} \end{bmatrix} = \begin{bmatrix} \cos\omega_0 & -\sin\omega_0 \\ \sin\omega_0 & \cos\omega_0 \end{bmatrix} \begin{bmatrix} b_{Ri} \\ b_{Ii} \end{bmatrix} \tag{15}$$

where ω_0 is the center frequency of the required complex bandpass filter $(-\pi \le \omega_0 < \pi)$ and $\bar{a}'_i = a'_{Ri} + ja'_{Ii}$, $\bar{b}'_i = b'_{Ri} + jb'_{Ii}$ are the rotated zeros and poles. The $\bar{a}'_i$ and $\bar{b}'_i$ from (15) are substituted into (14) to determine the complex coefficients $\bar{p}_i$ and $\bar{q}_i$ of the complex LDE in the form

$$Y(\omega_1, \omega_2, n_3) = q_0^{-1}\left[\sum_{i=0}^{M-1} \bar{p}_i X(\omega_1, \omega_2, n_3 - i) - \sum_{i=1}^{N-1} \bar{q}_i Y(\omega_1, \omega_2, n_3 - i)\right]. \tag{16}$$

Example: 3-D FP Filters using Real- Versus Complex-Coefficient Bandpass LDE Filters

A digitized video image sequence $x(n_1, n_2, n_3)$ containing moving vehicles has been obtained and consists of 155 frames of dimension 128 × 128. The 130th frame $x(n_1, n_2, 130)$ is shown in Fig. 3. Two vehicles are shown traveling at the same velocity from the right side to the left side in the far lane of traffic along with a single vehicle traveling at approximately the same velocity, but opposite direction, in the near lane of traffic. A 3-D combined DFT/LDE FP filter has been designed to enhance the two vehicles in the far lane, using *real-coefficient* LDE's and having a passband plane P_1, given by $-0.71\omega_1 + 0.08\omega_2 + \omega_3 = 0$. The vehicle in the near lane, however, has most of its energy in the plane P_2, given by $-0.71\omega_1 + 0.08\omega_2 - \omega_3 = 0$. Consequently, all three vehicles appear in the output $y(n_1, n_2, 130)$, as shown in Fig. 4. A corresponding 3-D combined DFT/LDE FP filter has been designed with *complex-coefficient* LDE's. The complex LDE's are of order $M = N = 2$ and have been obtained from a second-order Butterworth low-pass prototype filter. The magnitude frequency response $M(\omega_1, \omega_2, \omega_3)$ on ω_3 and the coefficients $\bar{p}_i$ and $\bar{q}_i$ of one such complex filter are shown in Fig. 5 for the 2-tuple $(\omega_1, \omega_2) = (-\pi/2, -\pi/2)$. The passband is on plane P_1 with $\omega_0 = -0.315\pi$ and $B = 0.0378\pi$. The 130th frame $y(n_1, n_2, 130)$ in the output of

Fig. 3. Single frame obtained from a digitized video image sequence containing moving vehicles.

Fig. 4. Filtered output using real-coefficient LDE's.

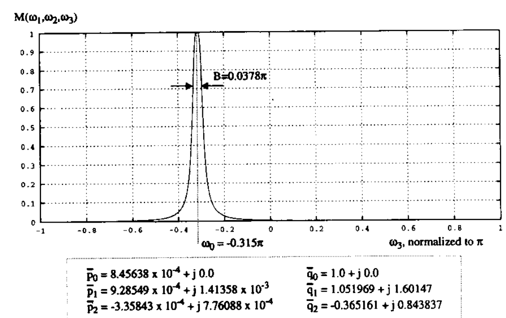

Fig. 5. Coefficients and magnitude response for complex filter used at 2-tuple $(-0.5\,\pi, -0.5\,\pi)$.

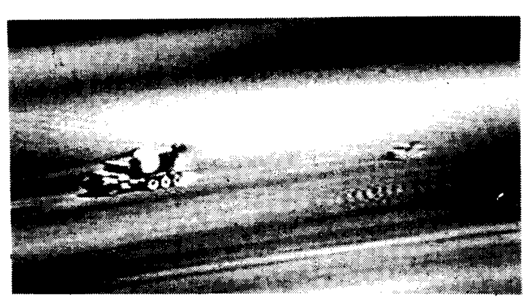

Fig. 6. Filtered output using complex-coefficient LDE's.

the 3-D combined DFT/LDE with complex-coefficient bandpass LDE's is shown in Fig. 6, where it is observed that *the time-reversed vehicle in the near lane has been successfully attenuated, due to the elimination of the passband plane* P_2.

IV. Summary

Real-coefficient LDE's impose symmetries in $H(j\omega_1, j\omega_2, j\omega_3)$ that leave just two independent octants in Ω^3. These symmetries imply that the 3-D combined DFT/LDE filter enhances signals and their time-reversed versions in the same way. This limitation may be overcome by employing complex-coefficient LDE filters, which allow four independent octants of $H(j\omega_1, j\omega_2, j\omega_3)$. Conventional methods of 3-D-DFT filtering and 3-D-LDE filtering also have four independent octants in $H(j\omega_1, j\omega_2, j\omega_3)$, where $\omega_1, \omega_2, \omega_3 \epsilon \mathbb{Z}$ in the former case and $\omega_1, \omega_2, \omega_3 \epsilon \mathbb{R}$ in the latter case.

References

[1] A. Choudhury and L. T. Bruton, "Multidimensional filtering using combined discrete Fourier transform and linear difference equation methods," *IEEE Trans. Circuits Syst.*, vol. 37, pp. 223–231, Feb. 1990.

[2] D. E. Dudgeon and R. M. Mersereau, *Multidimensional Digital Signal Processing*. Englewood Cliffs, NJ: Prentice-Hall, 1984, pp. 67–69.

[3] V. Rajaravivarma, P. K. Rajan, and H C. Reddy, "Symmetry study on 2-D complex analog and digital filter functions," *Multidimensional Syst. and Signal Processing*, vol. 2, pp. 161–187, 1991.

[4] L. T. Bruton and N. R. Bartley, "Three-dimensional image processing using the concept of network resonance," *IEEE Trans. Circuits Syst.*, vol. CAS-32, pp. 664–672, July 1985.

[5] A. S. Sedra, M. N. Snelgrove, and R. Allen, "Complex analog bandpass filters designed by linearly shifting real low-pass prototypes," in *Proc. IEEE Int. Symp. Circuits Syst.*, Kyoto, Japan, June 1985, pp. 1223–1226.

On the Uncertainty Principle in Discrete Signals

Léon Claude Calvez and Pierre Vilbé

Abstract—**It has recently been shown that the uncertainty principle holds true by appropriate definitions of the durations even if discrete signals are considered. A nice basic inequality was derived in the particular case where the Fourier transform is real. As an extension to this work, it is the purpose of this paper to prove the uncertainty relation in the general case of a complex Fourier transform and with somewhat extended definitions of durations.**

The existence of basic limitations on the possibility of simultaneously confining the time and frequency spread of analog signals is known as the Uncertainty Principle, a term borrowed from quantum mechanics. The existence of similar limitations in discrete signals has recently been investigated by Ishii and Furukawa [1].

In this paper, for continuity and brevity, formulas and nomenclature follow directly from the development in [1]. As in [1], consider a band-limited analog signal $f_a(t)$ whose Fourier transform $F_a(j\Omega)$ is

$$F_a(j\Omega) = 0, \quad \text{for } |\Omega| > \sigma.$$

Manuscript received August 23, 1991. This paper was recommended by Associate Editor Y. C. Lim.

The authors are with the Laboratoire d'Electronique et Systèmes de Télécommunications, Université de Bretagne Occidentale, 29287 Brest, Cédex, France.

IEEE Log Number 9201027.

Let a sequence $f(n) = f_a(nT)$ be the sample values of $f_a(t)$, where $T = \pi/\sigma$. The Fourier transform and the inverse Fourier transform are expressed by the following equations:

$$F(e^{j\omega}) = \sum_{n=-\infty}^{\infty} f(n) e^{-j\omega n} \tag{1}$$

$$f(n) = \frac{1}{2\pi} \int_{-\pi}^{\pi} F(e^{j\omega}) e^{j\omega n}\, d\omega \tag{2}$$

where $\omega = \Omega T$. The Fourier transforms are related by the relationship

$$F(e^{j\omega}) = F_a(j\Omega)/T, \quad |\omega| \le \pi. \tag{3}$$

Assuming that the energy of the signal is equal to 1, i.e.,

$$\sum_{n=-\infty}^{\infty} |f(n)|^2 = \frac{1}{2\pi} \int_{-\pi}^{+\pi} |F(e^{j\omega})|^2\, d\omega = 1 \tag{4}$$

we define the (time) spread D_n of $f(n)$ by

$$D_n^2 \triangleq \sum_{n=-\infty}^{\infty} (n - n_0)^2 |f(n)|^2 \tag{5}$$

and the (frequency) spread D_ω of $F(e^{j\omega})$ by

$$D_\omega^2 \triangleq \int_{-\pi}^{+\pi} (\omega - \omega_0)^2 |F(e^{j\omega})|^2\, d\omega \tag{6}$$

where n_0 and ω_0 are real numbers. It is worth noting that several analytical definitions of duration have been suggested in the past for analog signals and recently for discrete signals [1]; for a convenient choice of n_0 and ω_0, within a multiplicative constant, the above definitions of D_n and D_ω can be given an interesting interpretation [2]. If $n_0 = \omega_0 = 0$, they reduce to those of [1]. It is a standard exercise to show that when $|f(n)|$ is an even function of n, then $n_0 = 0$ minimizes (5), and that when $f(n)$ is real, then $|F(e^{j\omega})|^2$ is an even function of ω and $\omega_0 = 0$ minimizes (6).

In the *particular case where* $F(e^{j\omega})$ *is real* (a serious restriction), Ishii and Furukawa [1] have shown that the nice inequality

$$D_n D_\omega > \sqrt{\frac{\pi}{2}} \tag{7}$$

holds for $n_0 = \omega_0 = 0$ provided that $F_a(j\Omega) = 0$ for $|\Omega| = \sigma$. As an extension to this work we shall prove that the uncertainty relation (7) holds for *any complex Fourier transform* $F(e^{j\omega})$ *and for any choice of* n_0 *and* ω_0, provided that $F_a(j\Omega) = 0$ for $|\Omega| = \sigma$. This can be proved as follows.

Consider the integral

$$I \triangleq \int_{-\pi}^{+\pi} (\omega - \omega_0) \Phi(\omega)^* \Phi'(\omega)\, d\omega \tag{8}$$

where superscript * stands for complex conjugate and

$$\Phi(\omega) \triangleq e^{j\omega n_0} F(e^{j\omega}) \tag{9}$$

$$\Phi'(\omega) \triangleq \frac{d\Phi(\omega)}{d\omega}.$$

Integration by parts yields

$$I = K - \int_{-\pi}^{+\pi} \Phi(\omega)\left[\Phi(\omega)^* + (\omega - \omega_0)\Phi'(\omega)^*\right] d\omega \tag{10}$$

with

$$\begin{aligned} K &= \left[(\omega - \omega_0)|F(e^{j\omega})|^2\right]_{-\pi}^{+\pi} \\ &= \pi\left[|F(e^{j\pi})|^2 + |F(e^{-j\pi})|^2\right] \\ &\quad - \omega_0\left[|F(e^{j\pi})|^2 - |F(e^{-j\pi})|^2\right]. \end{aligned} \tag{11}$$